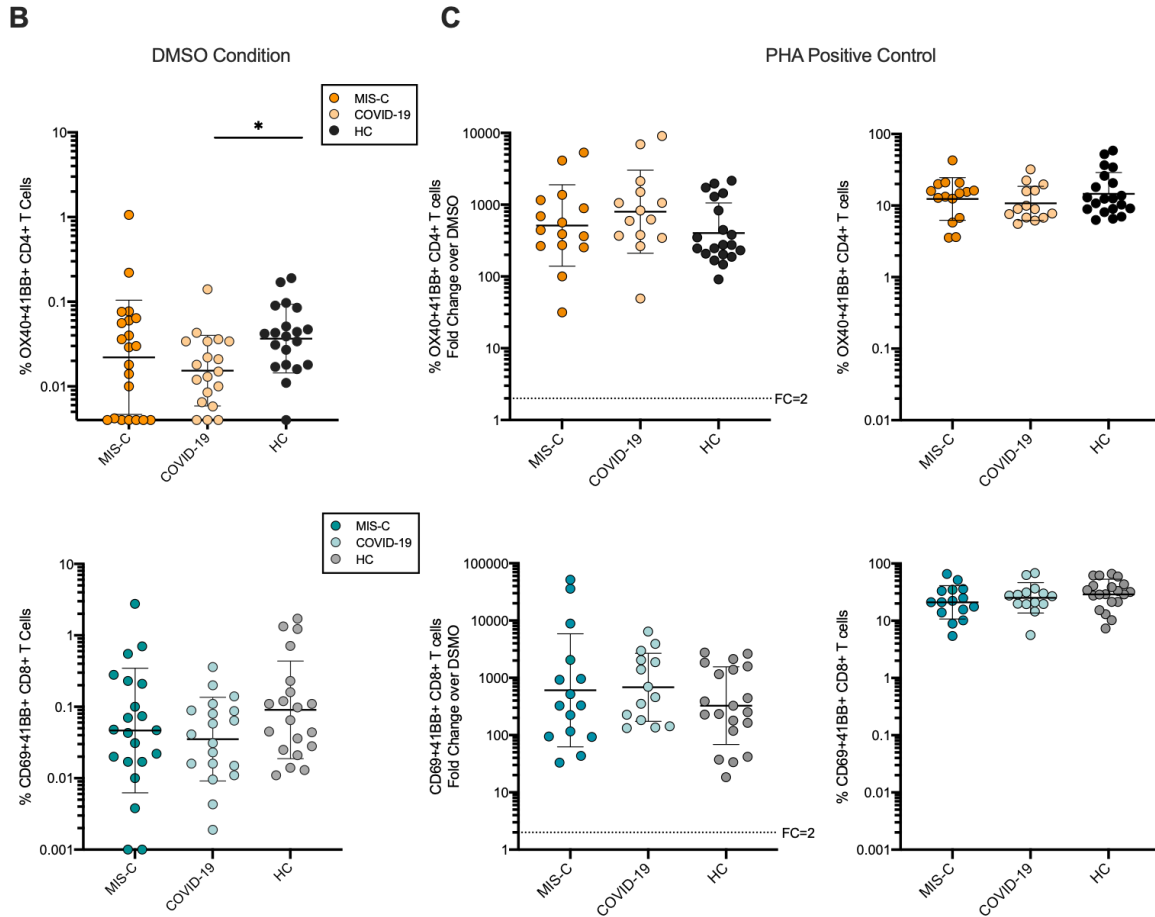
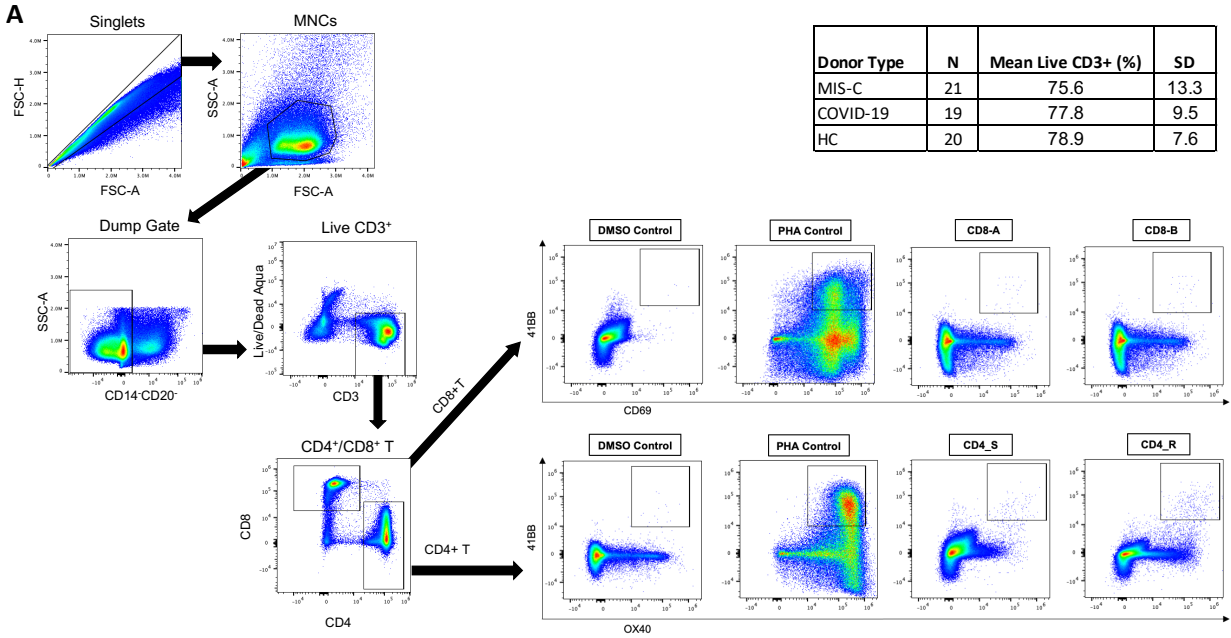


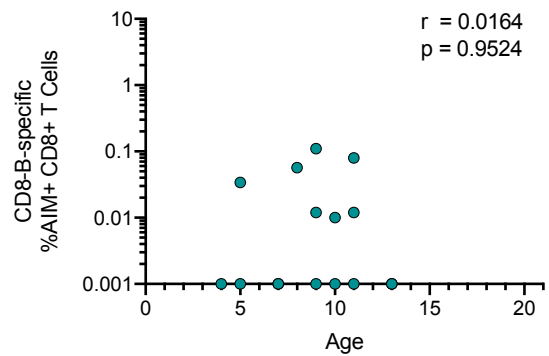
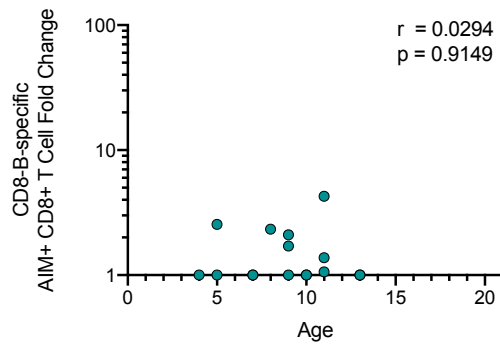
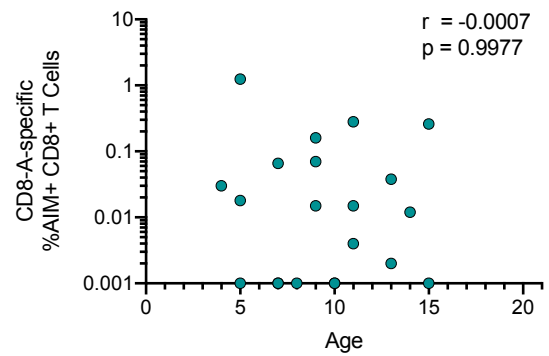
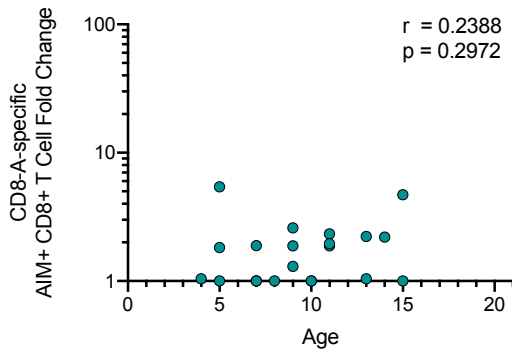
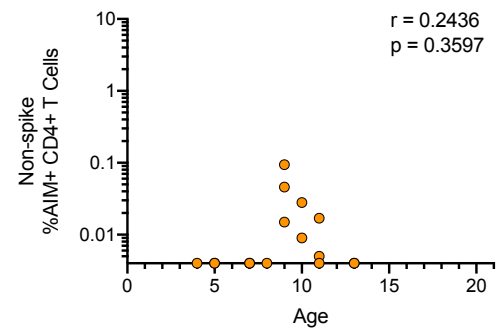
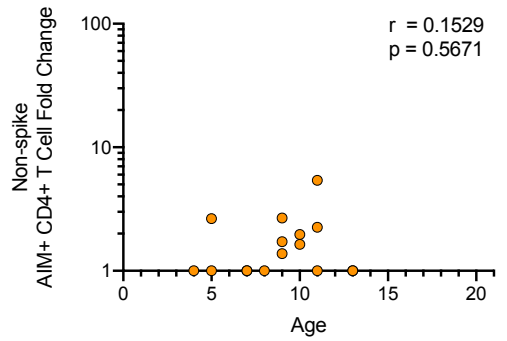
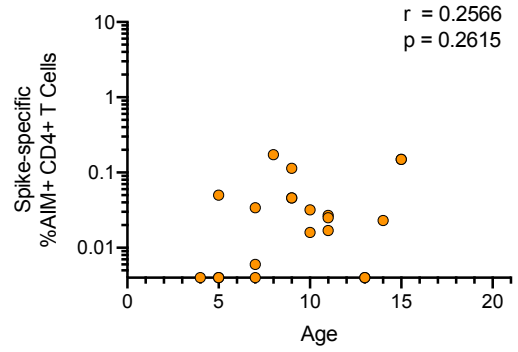
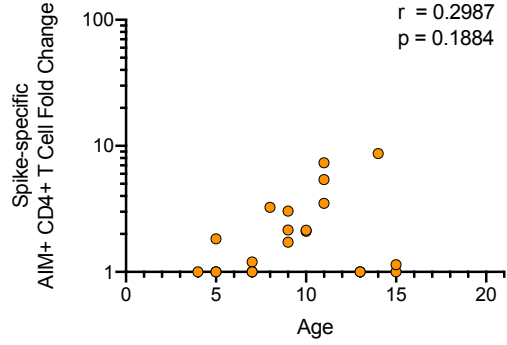
# Supplemental Information Figure S1.

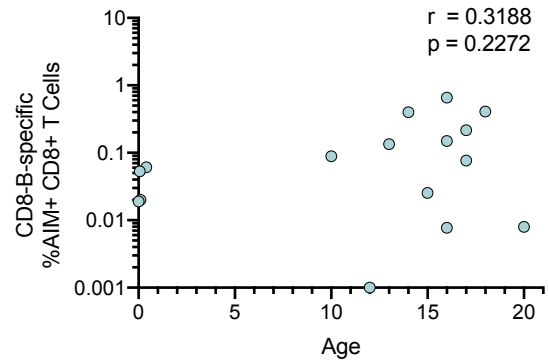
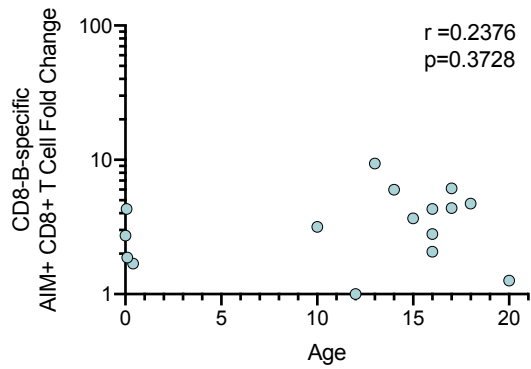
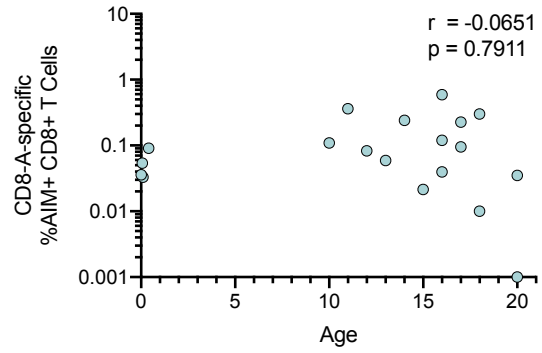
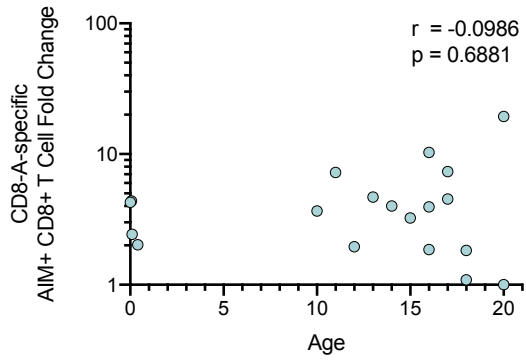
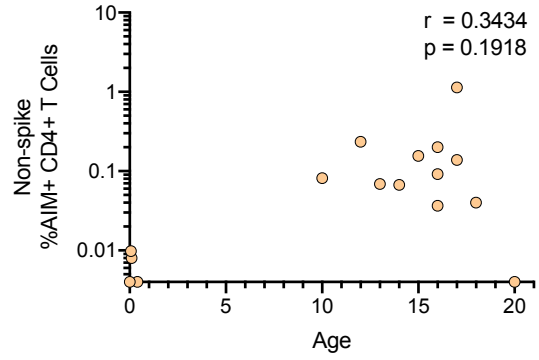
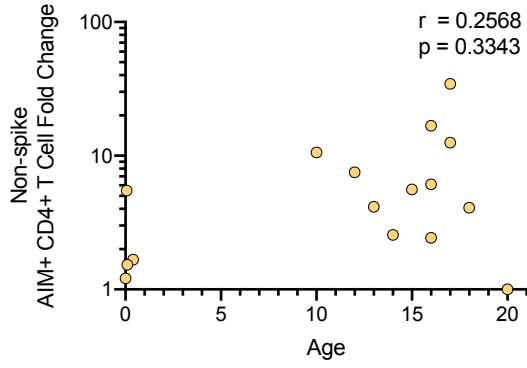
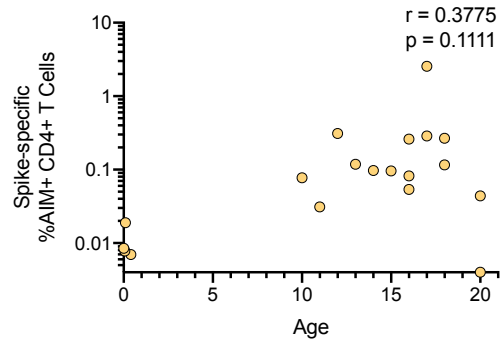
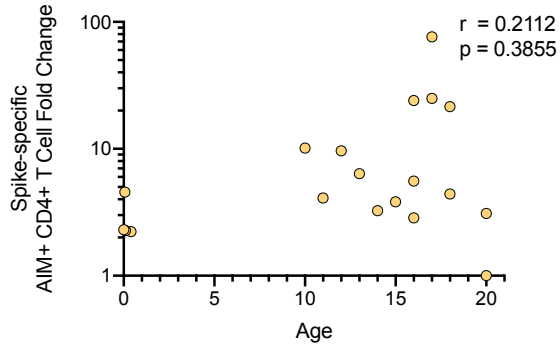


**Figure S1. AIM Assay Gating Strategy and Controls.** (A) Representative gating strategy to determine frequency of live CD4<sup>+</sup> and CD8<sup>+</sup> T-cells after DMSO negative control, PHA positive control, and peptide MP stimulation conditions. A convalescent COVID-19 participant is shown. Table shows mean T-cell viabilities in AIM assay across donors (% of live CD3<sup>+</sup> T-cells). No significant differences found by Kruskal-Wallis test. (B) T-cell responses to negative control condition DMSO in MIS-C, convalescent COVID-19, and healthy children (HC) shown as frequency of OX40<sup>+</sup>41BB<sup>+</sup>CD4<sup>+</sup> and CD69<sup>+</sup>41BB<sup>+</sup> CD8<sup>+</sup> T-cells; MIS-C (n=21), COVID-19 (n=19), and HC (n=20). (C) T-cell responses to positive control stimulation with PHA shown as OX40<sup>+</sup>41BB<sup>+</sup>CD4<sup>+</sup> and CD69<sup>+</sup>41BB<sup>+</sup>CD8<sup>+</sup> T-cell fold change (FC) over DMSO (L plots) and frequency with DMSO subtraction (R plots); MIS-C (n=15), COVID-19 (n=14), and HC (n=20). Geometric mean and geometric mean standard deviation (SD) shown, and only those with statistically significant relationships by Kruskal-Wallis test shown. \* p<0.05.

Figure S2.

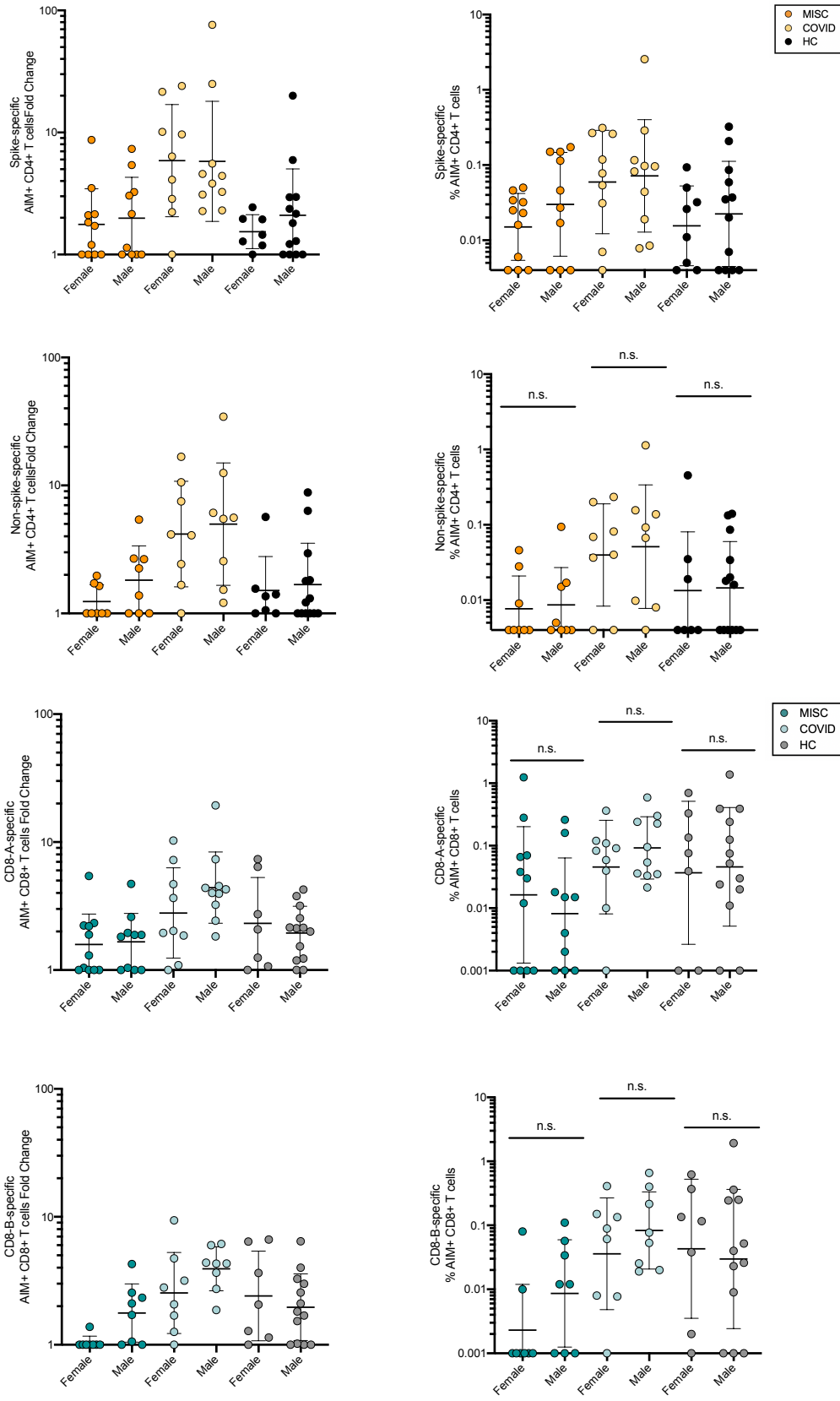
A



**B**

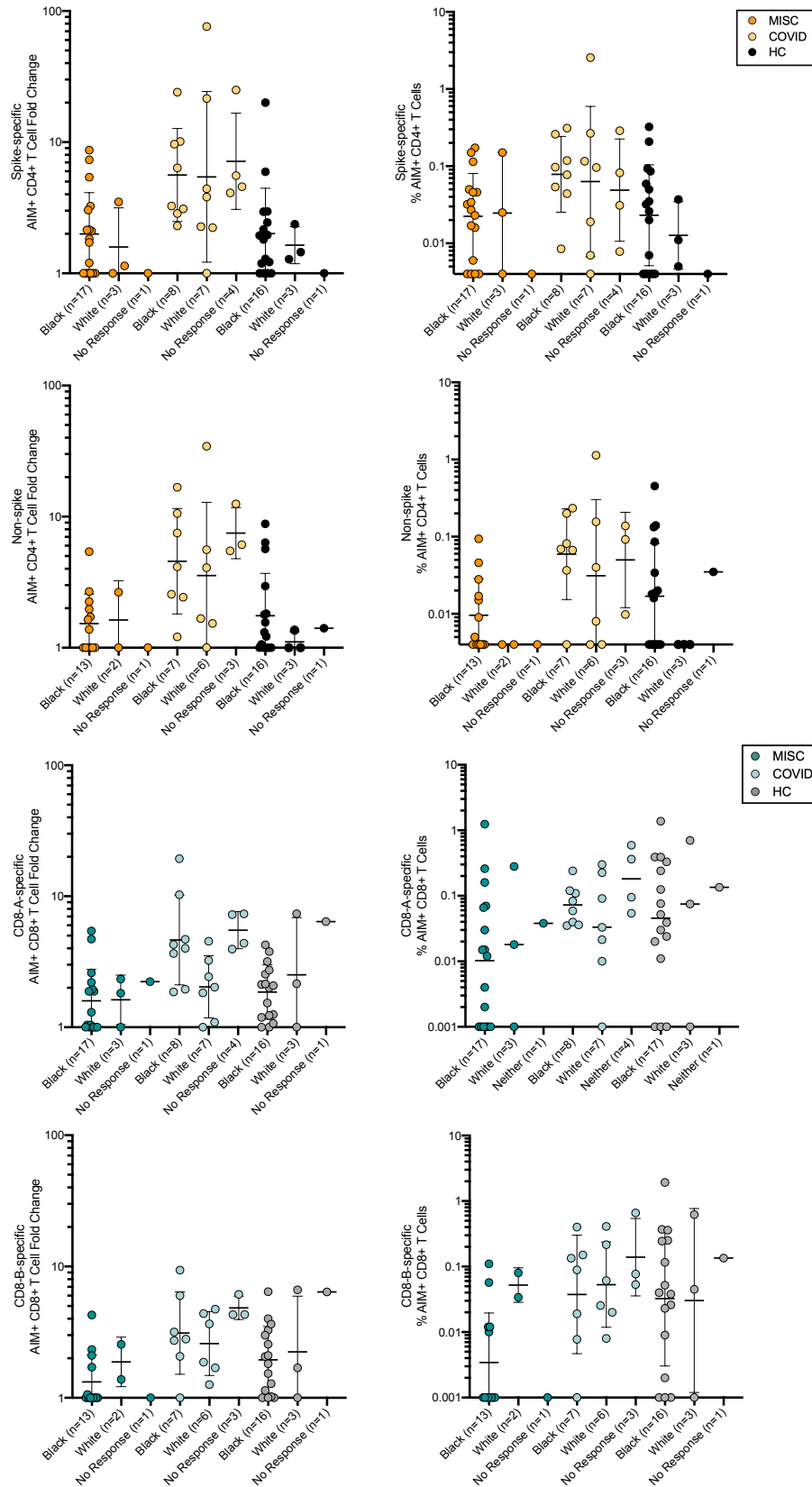
**Figure S2. Correlation of T-cell Responses by Age.** Relationship between SARS-CoV-2-specific CD4+ (Top) and CD8+ (Bottom) T-cell responses by both fold change (L plots) and frequency (R plots) and age for (A) MIS-C and (B) convalescent COVID-19. Statistical relationships were assessed with Spearman's correlation.

Figure S3.



**Figure S3. Distribution of T-cell Responses by Sex.** SARS-CoV-2-specific CD4+ (Top) and CD8+ (Bottom) T-cell responses by male and female sex shown as both fold change (L plots) and frequency (R plots). Geometric mean and geometric mean standard deviation (SD) shown with statistical comparison by Kruskal-Wallis test. No significant differences by sex were observed within donor types.

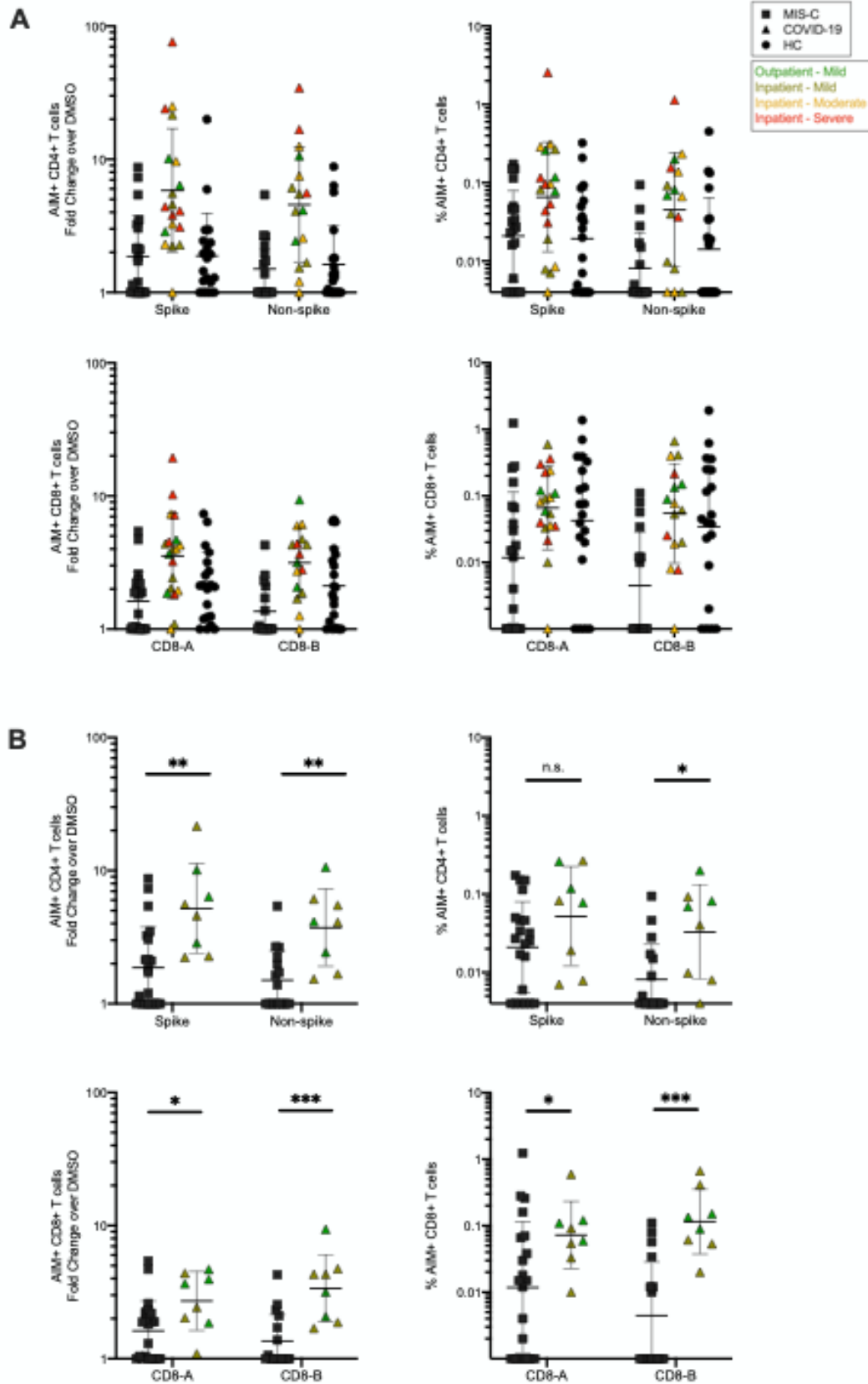
Figure S4.





**Figure S4. Distribution of T-cell Responses by Race.** SARS-CoV-2-specific CD4+ (Top) and CD8+ (Bottom) T-cell responses by Black, White, or No Response shown as both fold change (L plots) and frequency (R plots). Geometric mean and geometric mean standard deviation (SD) shown with statistical comparison by Kruskal-Wallis test. No significant racial differences were observed within donor type.

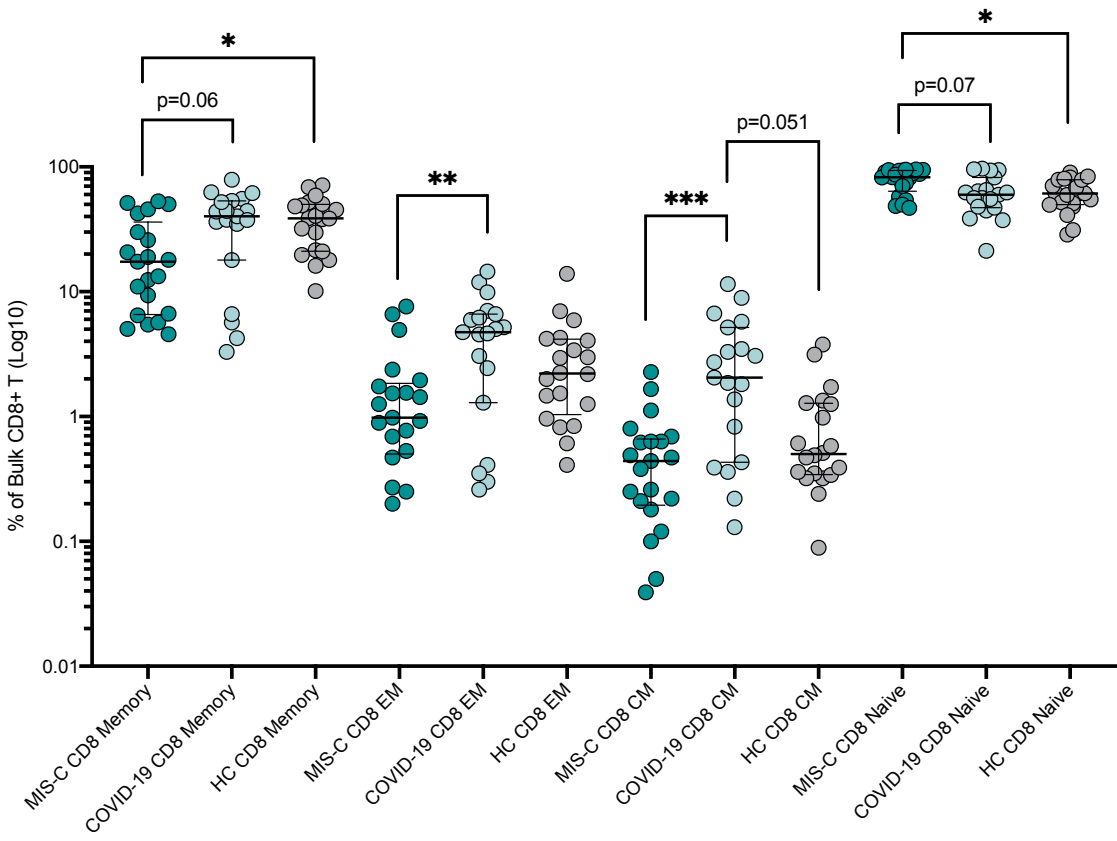
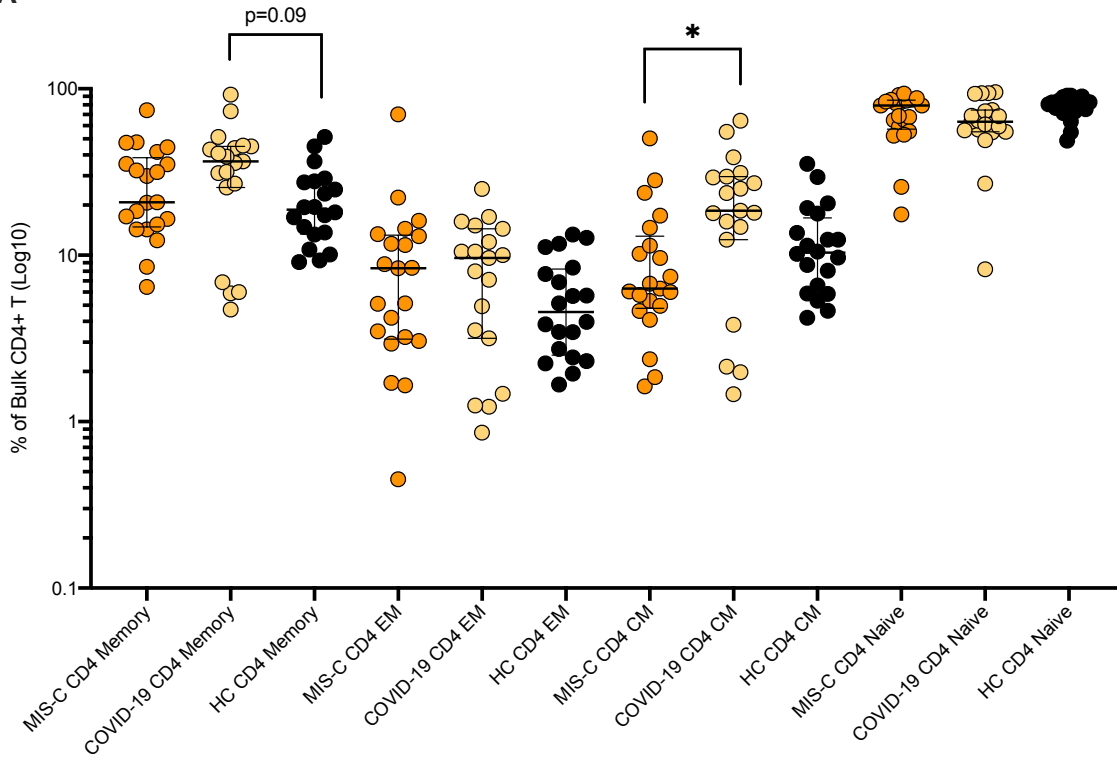
Figure S5.

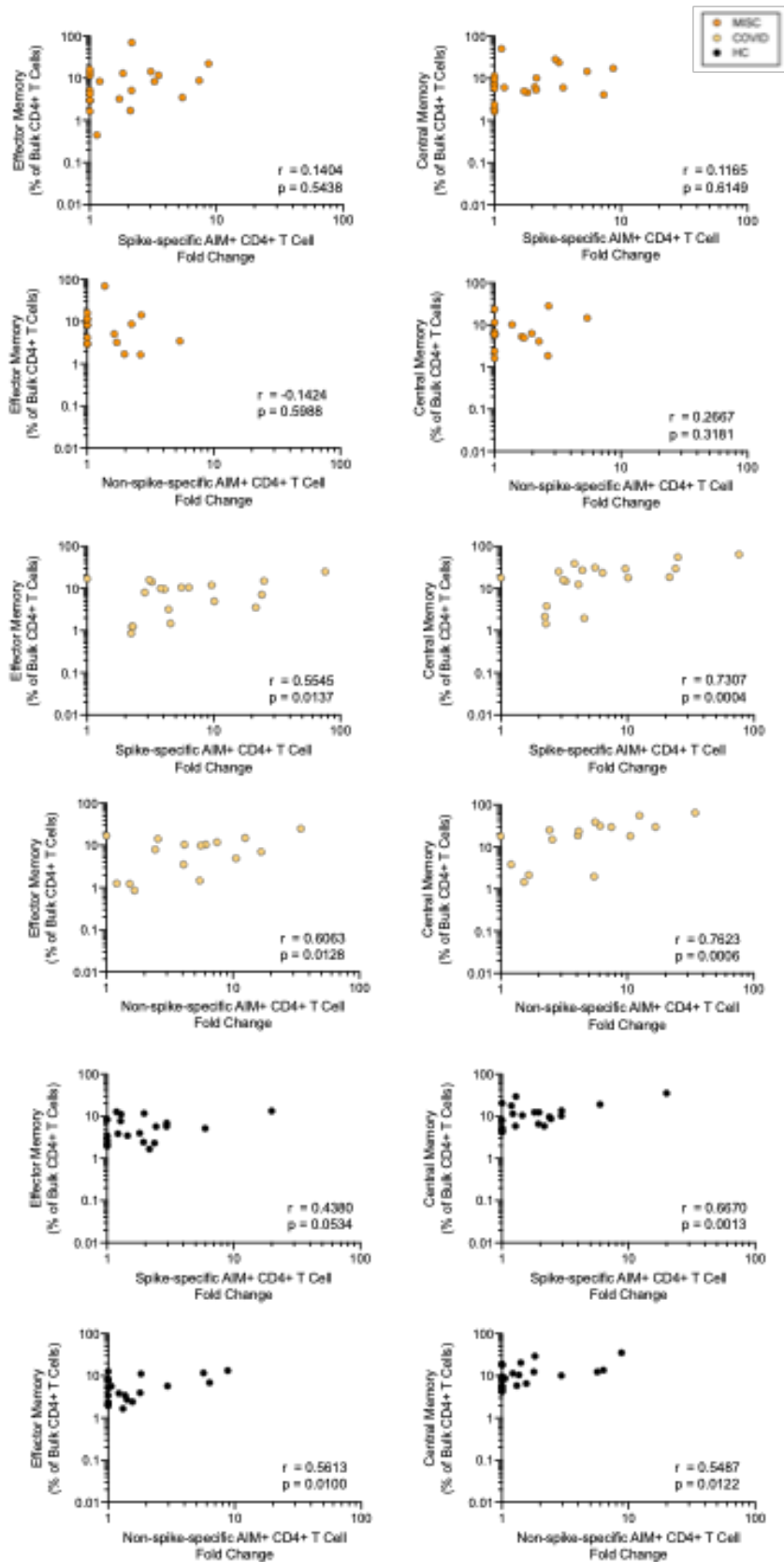


**Figure S5. T-cell Responses by COVID-19 Disease Severity.** (A) SARS-CoV-2-specific CD4+ and CD8+ T-cell responses (L plots, fold change [FC]; R plots, frequency) by peptide MP and COVID-19 disease severity (categorization defined in Methods). (B) T-cell response data for MIS-C (n=21) and mild COVID-19 (n=8) participants with FC (L plots) and frequency (R plots) shown. Line indicates geometric mean and geometric mean SD. Statistical comparisons conducted with Mann Whitney test. \*  $p < 0.05$ , \*\*  $p < 0.01$ , \*\*\*  $p < 0.001$ .

Figure S6.

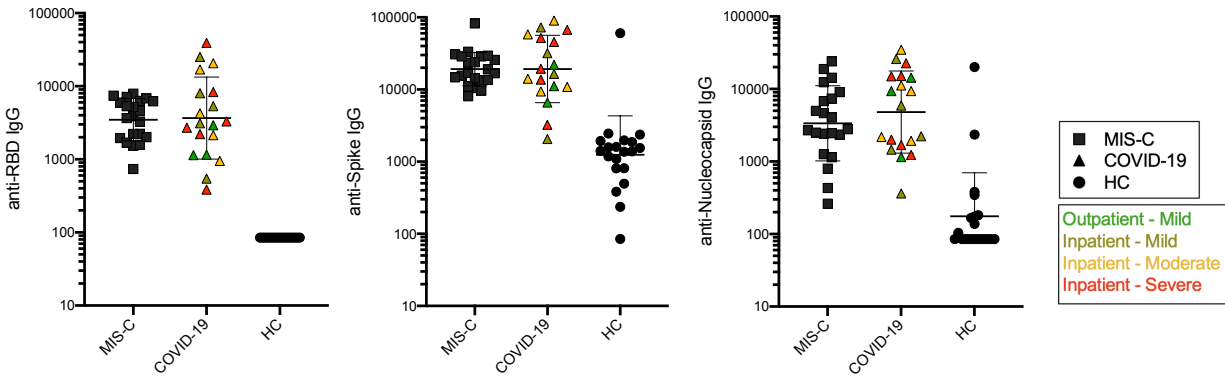
A



**B**

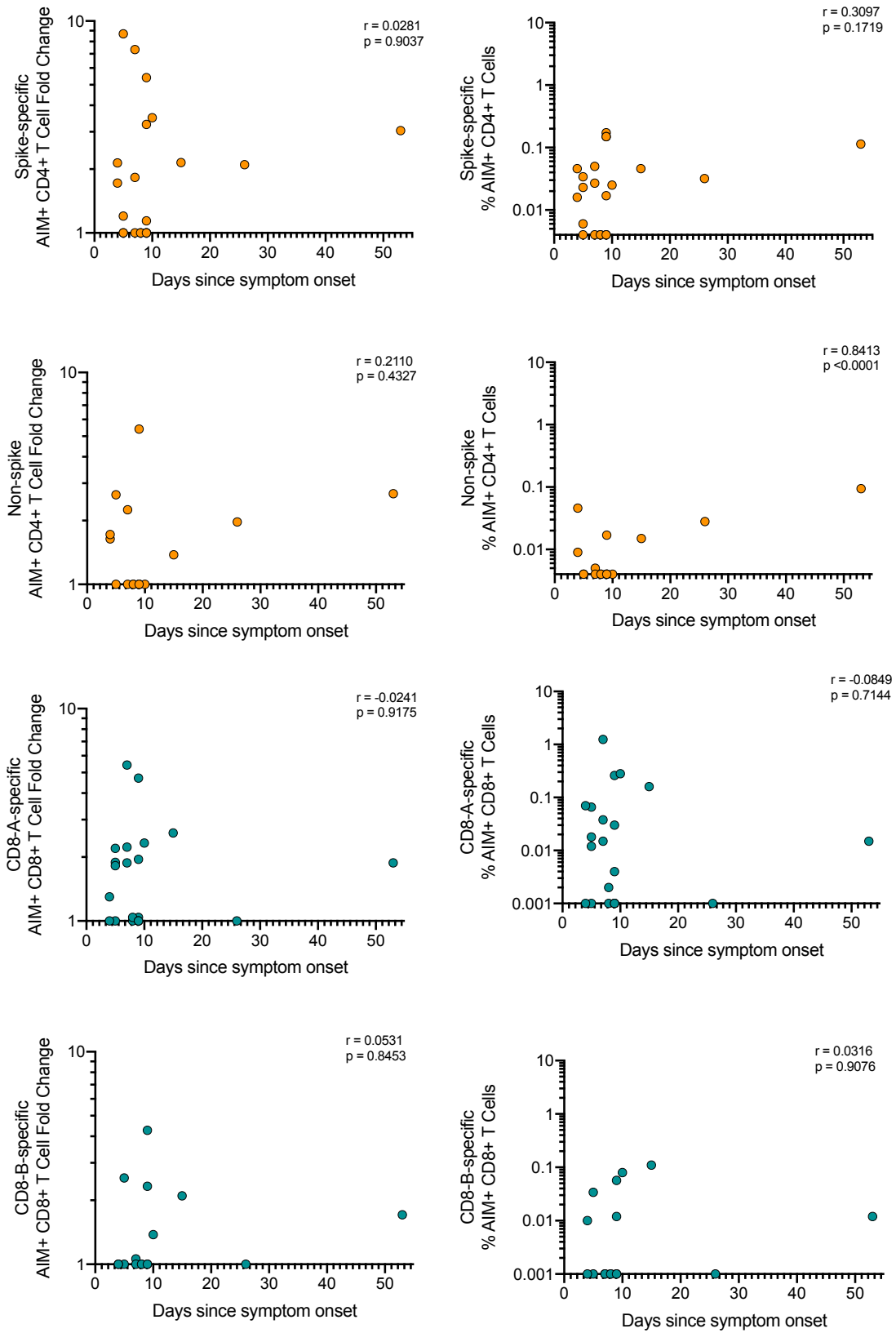
**Figure S6. Distribution of T-cell Subsets by Donor.** (A) Bulk CD4<sup>+</sup> and CD8<sup>+</sup> T-cell memory, effector memory (EM: CCR7-CD45RA<sup>-</sup>), central memory (CM: CCR7+CD45RA<sup>-</sup>), and naïve (CCR7+CD45RA<sup>+</sup>) T-cells shown as proportions of respective bulk CD4<sup>+</sup> and CD8<sup>+</sup> T-cells. Median and interquartile range shown with statistical comparison by Kruskal-Wallis test. \*  $p < 0.05$ , \*\*  $p < 0.01$ , \*\*\*  $p < 0.001$ . (B) Relationships between SARS-CoV-2-specific CD4<sup>+</sup> T-cell responses (fold change) and EM and CM CD4<sup>+</sup> T-cell subsets among MIS-C (Top), convalescent COVID-19 (Middle), and HC (Bottom) donors. Statistical relationships were assessed with Spearman's correlation.

Figure S7.



**Figure S7. Serologic Responses by COVID-19 Disease Severity.** Antibody titers to SARS-CoV-2 RBD, full-length spike, and nucleocapsid protein are shown with COVID-19 disease severity indicated (categorization defined in Methods). The line indicates geometric mean and geometric mean SD.

Figure S8.





**Figure S8. Correlation of T-cell Responses by Days since Symptom Onset in MIS-C Patients.** Relationship between SARS-CoV-2-specific CD4+ (Top) and CD8+ (Bottom) T-cell responses by both fold change (L plots) and frequency (R plots) and days since symptoms onset MIS-C (n=21). Statistical relationships were assessed with Spearman's correlation.

Figure S9.

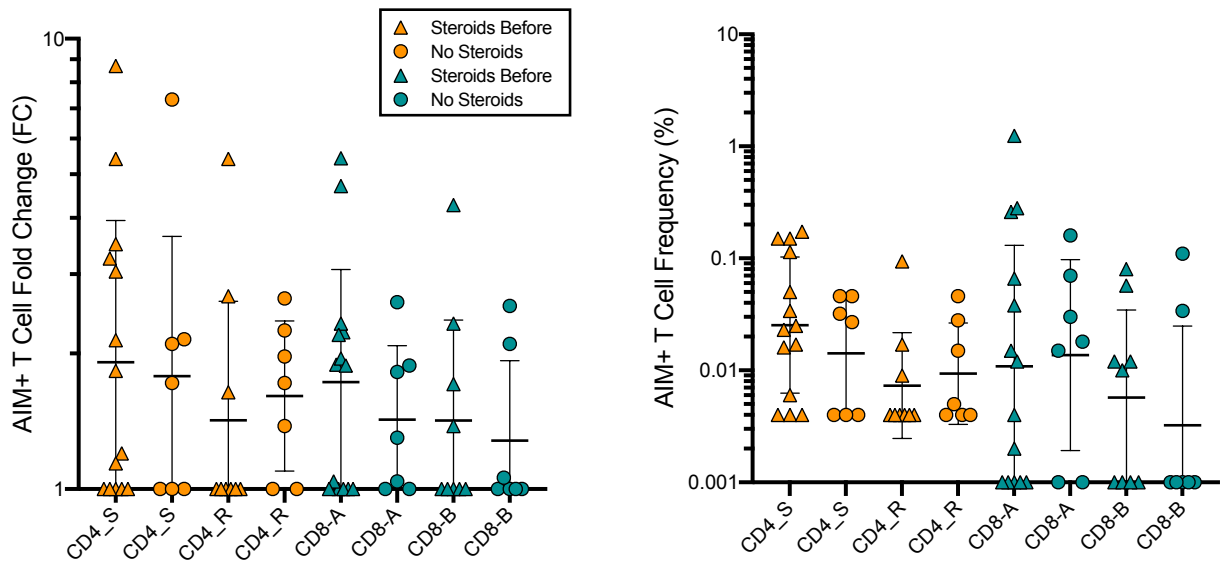


**Figure S9. Distribution of T-cell Responses by Steroid Treatment in MIS-C Patients.** SARS-CoV-2-specific CD4+ and CD8+ T-cell responses by those who received steroids prior enrollment (n=14) and those who did not (n=7) shown as both fold change (L plots) and frequency (R plots). Geometric mean and geometric mean standard deviation (SD) shown with statistical comparison by Kruskal-Wallis test. No significant differences were observed within MPs by steroid treatment.